ResearchGate

See discussions, stats, and author profiles for this publication at: https://www.researchgate.net/publication/319969085

Techno economic design of a solid oxide electrolysis system with solar thermal steam supply and thermal energy storage for the generation of renewable hydrogen

Article *in* International Journal of Hydrogen Energy · September 2017

DOI: 10.1016/j.ijhydene.2017.08.192

CITATIONS
19

READS
464

4 authors, including:

Henrik von Storch
Heliokon GmbH
36 PUBLICATIONS **390** CITATIONS
SEE PROFILE

Aziz Nechache
Engie
15 PUBLICATIONS **156** CITATIONS
SEE PROFILE

Some of the authors of this publication are also working on these related projects:

Project Methanol Production via Solar Reforming of Methane View project

Project ATLAS-MHC View project

All content following this page was uploaded by Aziz Nechache on 08 May 2019.

The user has requested enhancement of the downloaded file.

INTERNATIONAL JOURNAL OF HYDROGEN ENERGY XXX (2017) 1–11

Available online at www.sciencedirect.com

ScienceDirect

journal homepage: www.elsevier.com/locate/he

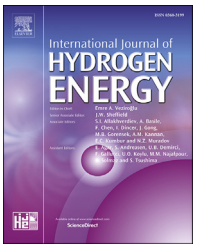

Techno economic design of a solid oxide electrolysis system with solar thermal steam supply and thermal energy storage for the generation of renewable hydrogen

M. Seitz [a], H. von Storch [b,*], A. Nechache [a], D. Bauer [a]

[a] German Aerospace Center (DLR), Institute of Engineering Thermodynamics, Pfaffenwaldring 38-40, 70569 Stuttgart, Germany

[b] German Aerospace Center (DLR), Institute of Solar Research, Professor-Rehm-Straße 1, 52428 Jülich, Germany

ARTICLE INFO

Article history:
Received 19 June 2017
Received in revised form
23 August 2017
Accepted 27 August 2017
Available online xxx

Keywords:
Power-to-Gas
Solid oxide electrolysis system
Direct steam generation
Latent heat thermal energy storage
Phase change material
Economic yield assessment

ABSTRACT

The dependency of renewable energy systems on environmental influences such as sun or wind availability is one of the greatest challenges in the energy transition. For this purpose, it is important to develop electro chemical storage systems for long-term storing of renewable electricity in the form of hydrogen or methane. In the presented work, an electrolysis system with solid-oxide electrolyser stacks is designed. A solar thermal receiver is used to produce the steam supplied to the electrolyser stacks. On the other hand, a thermal energy storage, using a phase change material, is used for the extension of the operational hours during the night time. The system is optimized to minimize the levelized costs of hydrogen and compared to a system without a thermal energy storage. Finally, the cost sensitivity for the four main components of the cost structure is evaluated and discussed.

© 2017 Hydrogen Energy Publications LLC. Published by Elsevier Ltd. All rights reserved.

Introduction

The production of hydrogen is a suitable possibility for storing renewable energy from wind farms or photovoltaic systems for a medium to long-term period, i.e. in the range from a few days up to several months. For this purpose, an electrolysis system is used for the generation of hydrogen. This hydrogen can be used for the mobility sector, basic material chemistry and can be fed into the gas grid in form of hydrogen or methane. As the last option, it is also possible to use the storage capacity of the gas grid for a shifted supply of

Abbreviations: ASR, Area specific resistance; CAPEX, Capital expenditures; CSP, Concentrating solar power; DNI, Direct normal irradiance; EPC, Engineering-procurement-construction; HHV, Higher heating value; HTF, Heat transfer fluid; HTX, Heat exchanger; IAM, Incidence angle modifier; LCOH, Levelized costs of hydrogen; LHTES, Latent heat thermal energy storage; OPEX, Operational expenditures; PCM, Phase change material; SC, Steam conversion; SF, Solar field; SOEC, Solid oxide electrolysis cell; TES, Thermal energy storage; TMY, Typical meteorological year; TTD, Terminal temperature difference.

* *Corresponding author.*
E-mail address: Henrik.vonStorch@dlr.de (H. von Storch).

http://dx.doi.org/10.1016/j.ijhydene.2017.08.192
0360-3199/© 2017 Hydrogen Energy Publications LLC. Published by Elsevier Ltd. All rights reserved.

Please cite this article in press as: Seitz M, et al., Techno economic design of a solid oxide electrolysis system with solar thermal steam supply and thermal energy storage for the generation of renewable hydrogen, International Journal of Hydrogen Energy (2017), http://dx.doi.org/10.1016/j.ijhydene.2017.08.192

Nomenclature

a_{HL}	Heat loss parameter absorber ($W\,m^{-2}\,K^{-2}$)
A_{nom}	Nominal collector area (m^2)
A_{stack}	Active stack area (cm^2)
$\cos(\theta_i)$	Cosine losses of solar collector
C_{CAPEX}	Capital expenditures (EUR)
$C_{Electricity}$	Electricity costs (EUR a^{-1})
C_{LCOH}	Levelized costs of hydrogen (EUR kWh^{-1})
C_{OPEX}	operational expenditures (EUR a^{-1})
f_{AN}	Annuity factor
f_{ASR}	Area specific resistance factor ($\Omega\,cm^2$)
f_{foc}	Percentage of field in focus
f_{SC}	Steam conversation factor
F	Faraday constant ($96,485.34\ C\ mol^{-1}$)
G_{DNI}	Direct normal solar irradiance ($W\ m^{-2}$)
h_{HHV}	Higher heating value of hydrogen ($285,840\ J\ mol^{-1}$)
i	Interest rate (%)
j_{stack}	Current density ($A\,cm^{-2}$)
$K(\theta_i)$	Incidence angle modifier of solar collector
M	Molar mass ($kg\ kmol^{-1}$)
n	Payout time (a)
$\dot{n}$	Molar flow ($kmol\ s^{-1}$)
p	Partial pressure (bar)
p_{cell}	Average cell pressure (bar)
p_{std}	Pressure at standard conditions (1013.25 bar)
P	Electrical power (kW)
$\dot{Q}$	Heat flow (kW)
R	Universal gas constant ($8.314\ J\ mol^{-1}\ K^{-1}$)
T	Temperature (K)
T_{abs}	Average absorber temperature (K)
T_{cell}	Average cell temperature (K)
T_{env}	Temperature of the environment (K)
U_{nernst}	Nernst voltage (V)
x	Molar gas fraction
$\Delta_r G_T$	Gibbs free energy change of reaction
$\Delta_r H_T$	Enthalpy change of reaction
$\Delta_r S_T$	Entropy change of reaction
ε	Empiric value for area specific resistance calculation
η	Efficiency
θ_i	Incidence angle of solar collector

electrical energy by the use of renewable hydrogen in fossil fired power plants. The use of renewable electricity from the electricity grid by an electrolysis system extends the share of renewable energy sources.

One possible way for the realization of power-to-gas is the electrolysis of water to hydrogen using a solid oxide electrolysis cell (SOEC), as discussed by Gahleitner [1]. Working at high temperature (above 600 °C) allows: (i) providing part of the energy needed thermally and not electrically, possibly from waste heat, (ii) generating directly pure hydrogen in important quantities, (iii) using cheap catalyst such as nickel instead of expensive platinum (see the work of Nechache et al. [2]). In the work of Henke et al. [3] the behavior of a pressurized SOEC and the pressure dependency of the water electrolysis are described. It was concluded that with increasing pressure, more electrical energy is needed for the separation of hydrogen and oxygen. Sanz-Bermejo et al. [4] investigated three SOEC systems under several operational modes and part load conditions. They summarized that the system performance is maximized when the SOEC is operated with a constant steam conversion rate. The thermoneutral operational mode was identified to provide almost constant cell conversion efficiency over the complete operational range. Due to this operational mode, the temperature gradient between the inlet and the outlet of the SOEC at both the cathode and the anode is eliminated, which minimizes the thermal stress of the SOEC.

Coupling of a SOEC with concentrating solar power (CSP) power plant, like discussed in the work of Monnerie et al. [5], can reduce the electricity demand of the SOEC from the grid to less than 5% of the annual operating time. This approach requires a large CSP-Power plant and other renewable electricity can only be used in a small amount from the grid. Josi et al. [6] concluded in their work that an electrolyser coupled with a CSP system would achieve a higher exegetic efficiency and sustainability index compared to a photovoltaic system. One of the main problems of the SOEC is the integration options of an external steam supply, discussed by AlZahrani et al. [7]. The integration issue of a suitable steam supply was the main idea for the presented work.

This paper presents the techno-economic design of a SOEC system. Integrating solar thermal power aims at reducing the electrical power demand of the proposed system by the direct use of thermal energy from a solar field (SF) for the evaporation of preheated water. A thermal energy storage (TES) system is used for the enhancement of the annual hydrogen production of the electrolyser. By a parametric study, the optimal TES capacity and the SF size are determined by minimizing the levelized costs of hydrogen (LCOH). Finally a sensitivity study for the four main cost shares is presented and discussed in this paper. The designed system combines the advantages from CSP and SOEC systems to reach low LCOH and create a system which needs only a small SF and uses all kinds of renewable electricity from the grid. Additionally the impact of a new storage technology, which is currently under development, to the SOEC electrolysis system is evaluated and discussed.

Methods and system description

The SOEC system (see Fig. 1) is operated at its thermoneutral operational mode: both inlet and outlet temperatures of the cathode and anode streams are not modified by the chemical reaction and the electricity demand of the SOEC. The water provided is evaporated by a CSP receiver and is forwarded as saturated steam to the SOEC during the production of hydrogen from the SF. A latent heat thermal energy storage (LHTES) with a phase change material (PCM) is used to provide saturated steam during the night and cloudy periods. Renewable power from the electricity grid is used to power the SOEC. The generated hydrogen is dried, compressed and stored for different applications with hydrogen demand.

Please cite this article in press as: Seitz M, et al., Techno economic design of a solid oxide electrolysis system with solar thermal steam supply and thermal energy storage for the generation of renewable hydrogen, International Journal of Hydrogen Energy (2017), http://dx.doi.org/10.1016/j.ijhydene.2017.08.192

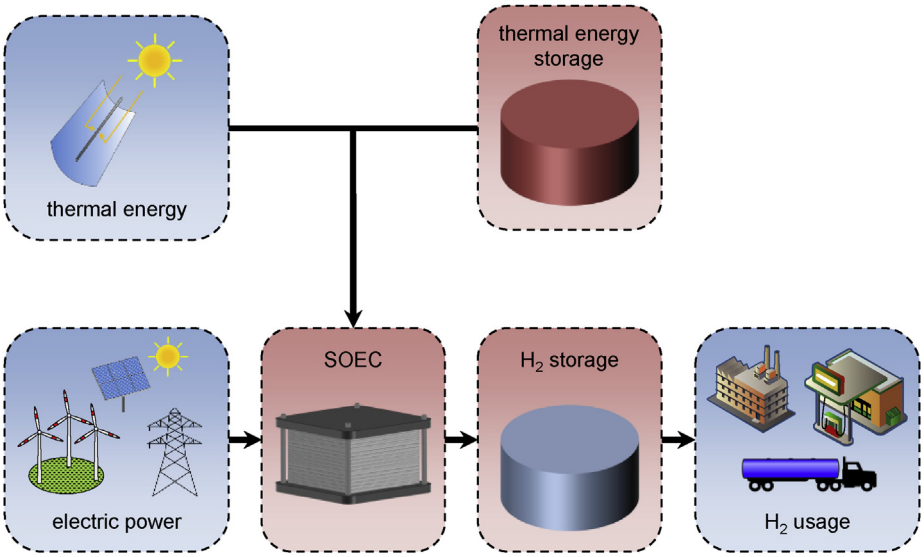

Fig. 1 – Schematics of a solar thermal powered SOEC system for the generation of renewable hydrogen with a thermal energy storage for the supply of saturated steam during the night time.

Background of solid oxide electrolysis cell

The electrolysis of water is an endothermic chemical reaction of water (H_2O) to oxygen (O_2) and hydrogen (H_2) and can be written as Eq. (1).

$$H_2O \rightarrow \frac{1}{2}O_2 + H_2 \tag{1}$$

The enthalpy change $\Delta_r H_T$ of this reaction is given by Eq. (2) as the sum of the Gibbs free energy change of reaction $\Delta_r G_T$ and the product of the entropy change of reaction $\Delta_r S_T$ and the temperature T.

$$\Delta_r H_T = \Delta_r G_T + T \cdot \Delta_r S_T \tag{2}$$

The temperature and pressure depended Nernst voltage U_{nernst} of a single SOEC, as for example described by Sanz-Bermejo et al. [4], is given by Eq. (3) and calculated by the Gibbs free energy change of reaction $\Delta_r G^0_{T_{cell}}$, the average cell temperature T_{cell}, the partial pressures of water p_{H_2O}, hydrogen p_{H_2} and oxygen p_{O_2}. The fraction of the pressure at standard conditions and the operational pressure inside the SOEC describes the pressure dependence of the Nernst voltage. The Faraday constant $F = 96,485.34\ C\ mol^{-1}$ and the universal gas constant $R = 8.314\ J\ mol^{-1}\ K^{-1}$.

$$U_{\text{nernst}} = \frac{\Delta_r G^0_{T_{cell}} - R \cdot T_{cell}}{2 \cdot F} \cdot ln\left(\frac{p_{H_2O}}{p_{H_2} \cdot \sqrt{p_{O_2}}} \cdot \sqrt{\frac{p_{std}}{p_{cell}}}\right) \tag{3}$$

The current density of the SOEC stack j_{stack} is calculated by the Nernst voltage U_{nernst}, the total electrical power of the stack P_{stack}, the active stack area A_{stack} and the area specific resistance factor f_{ASR} of the stack, as described in Eq. (4).

$$j_{\text{stack}} = -\frac{U_{\text{nernst}}}{2 \cdot f_{\text{ASR}}} + \sqrt{\left(\frac{U_{\text{nernst}}}{2 \cdot f_{\text{ASR}}}\right)^2 + \frac{P_{\text{stack}}}{A_{\text{stack}} \cdot f_{\text{ASR}}}} \tag{4}$$

The area specific resistance factor f_{ASR} describes all temperature dependent irreversible losses of the SOEC and is based on empirical measurements of real cells. Petipas et al. [8] proposed $\varepsilon = 0.25\ \Omega\ cm^2$ in Eq. (5) for a SOEC stack at an average cell temperature $T_{cell} = 1073K$, resulting in $f_{ASR} = 0.5\ \Omega\ cm^2$, based on the equations of Fu et al. [9].

$$f_{\text{ASR}} = \varepsilon + exp\left(\frac{4900}{T_{\text{cell}}} - 5.95\right) \tag{5}$$

With the results of Eq. (4), the molar flow of produced hydrogen $\dot{n}_{H_2,prod}$ can be calculated via Eq. (6).

$$\dot{n}_{H_2,prod} = \frac{j_{stack} \cdot A_{stack}}{2 \cdot F} \tag{6}$$

The molar flows $\dot{n}_{H_2O,in}$ and $\dot{n}_{H_2O,out}$ are calculated by the molar flow of produced hydrogen $\dot{n}_{H_2,prod}$ and the steam conversion (SC) factor f_{SC}.

$$\dot{n}_{H_2O,in} = \frac{\dot{n}_{H_2,prod}}{f_{SC}} \tag{7}$$

$$\dot{n}_{H_2O,out} = \dot{n}_{H_2O,in} - \dot{n}_{H_2,prod} \tag{8}$$

The SC factor f_{SC} describes the mole share of the produced hydrogen $\dot{n}_{H_2,prod}$ based on the inlet molar flow of water $\dot{n}_{H_2O,in}$. Common values for the SC factor are usually between 60%, proposed by the work of Sanz-Bermejo [4], and 80%, proposed by the work of Rivera-Tinoco et al. and Udagawa et al. [10,11]. For this work a medium value of 75%, based on the work of Petipas et al. [8], is assumed.

Based on the mass balance of the SOEC and Eq. (1), it is possible to calculate the molar flows at the inlet and the outlet of the SOEC, as described for the major components hydrogen and oxygen by Eq. (9)–(11). The mole fractions $x_{H_2,in} = 0.1$ and $x_{H_2O,in} = 0.9$ are assumed based on the work of Rivera-Tinoco

Please cite this article in press as: Seitz M, et al., Techno economic design of a solid oxide electrolysis system with solar thermal steam supply and thermal energy storage for the generation of renewable hydrogen, International Journal of Hydrogen Energy (2017), http://dx.doi.org/10.1016/j.ijhydene.2017.08.192

et al. [10] and the work of Udagawa et al. [11]. The molar flow of nitrogen $\dot{n}_{N_2,in}$ is not modified by the SOEC.

$$\dot{n}_{H_2,in} = \frac{x_{H_2,in}}{x_{H_2O,in}} \cdot \dot{n}_{H_2O,in} \quad (9)$$

$$\dot{n}_{H_2,out} = \dot{n}_{H_2,in} + \dot{n}_{H_2,prod} \quad (10)$$

$$\dot{n}_{O_2,out} = \dot{n}_{O_2,in} + \frac{1}{2} \cdot \dot{n}_{H_2,prod} \quad (11)$$

$$\dot{n}_{N_2,out} = \dot{n}_{N_2,in} \quad (12)$$

After the calculation of the mass balance, it is necessary to calculate the energy balance, as described by Eq. (13). The electrical power of the stack P_{stack} and the inlet heat flow $\dot{Q}_{in}$ are considered with a positive prefix (into the system boundary) and the chemical reaction heat flow $\dot{Q}_{reaction}$ and the outlet heat flow $\dot{Q}_{out}$ with a negative prefix (out of the system boundary). The heat losses of the SOEC were neglected for the presented calculations.

$$P_{stack} + \dot{Q}_{reaction} + \dot{Q}_{in} + \dot{Q}_{out} = 0 \quad (13)$$

The chemical reaction heat flow $\dot{Q}_{reaction}$ is calculated by the enthalpy change $\Delta_r H_T$ and the produced molar flow of hydrogen $\dot{n}_{H_2,prod}$, as described by Eq. (14).

$$\dot{Q}_{reaction} = \Delta_r H_T \cdot \dot{n}_{H_2,prod} \quad (14)$$

The heat flow at the inlet $\dot{Q}_{in}$ of the SOEC is calculated by both the cathode inlet flow $\dot{Q}_{cathode,in}$ and the anode inlet flow $\dot{Q}_{anode,in}$.

$$\dot{Q}_{in} = \dot{Q}_{cathode,in} + \dot{Q}_{anode,in} \quad (15)$$

$$\dot{Q}_{cathode,in} = \left(\dot{n}_{H_2,in} \cdot c_{p,H_2} + \dot{n}_{H_2O,in} \cdot c_{p,H_2O}\right) \cdot (T_{in} - T_{cell}) \quad (16)$$

$$\dot{Q}_{anode,in} = \left(\dot{n}_{N_2,in} \cdot c_{p,N_2} - \dot{n}_{O_2,in} \cdot c_{p,O_2}\right) \cdot (T_{in} - T_{cell}) \quad (17)$$

The heat flow at the outlet $\dot{Q}_{out}$ of the SOEC is calculated by almost the same way, using the negative cathode outlet flow $\dot{Q}_{cathode,out}$ and the anode outlet flow $\dot{Q}_{anode,out}$.

$$\dot{Q}_{out} = \dot{Q}_{cathode,out} + \dot{Q}_{anode,out} \quad (18)$$

$$\dot{Q}_{cathode,out} = \left(-\dot{n}_{H_2,out} \cdot c_{p,H_2} - \dot{n}_{H_2O,out} \cdot c_{p,H_2O}\right) \cdot (T_{cell} - T_{out}) \quad (19)$$

$$\dot{Q}_{anode,out} = \left(-\dot{n}_{N_2,out} \cdot c_{p,N_2} - \dot{n}_{O_2,out} \cdot c_{p,O_2}\right) \cdot (T_{cell} - T_{out}) \quad (20)$$

The given Eq. (3)–(20) for the calculation of the SOEC working parameters cannot be solved analytically. Therefore, an iterative solving algorithm is implemented in the mathematical model of the SOEC. Sanz-Bermejo et al. [4] and Petipas et al. [8] used a similar solving algorithm for the correct calculation of both the mass as well as the energy balance. This algorithm was used and implemented for the simulation work, presented in this paper. In a first step, the Nernst voltage U_{nerst} (see Eq. (3)) and the current density j_{stack}(see Eq. (4)) are calculated by estimating start values for the gas compositions x_{out} at the cathode and anode outlets of each substance and the average cell temperature

$$T_{cell} = \frac{T_{in} + T_{out}}{2} \quad (21)$$

of the SOEC, by assuming a new outlet temperature T_{out}. If the mass balance is solved successfully, a new stack outlet temperature T_{out} is calculated. The iterative loops are solved until they reach their convergence criteria. In this work, the SOEC is operated in a thermoneutral operational mode. This means that the inlet and the outlet temperatures T_{in} and T_{out} of the streams are equal to the cell temperature T_{cell}.

Solar thermal receiver for direct steam generation

The steam supplied to the SOEC is for the presented work assumed to be provided by the solar thermal receiver Euro-Trough with the absorber Schott PTR70 [12], as discussed in the work of Feldhoff et al. [13]. For the yield calculation the thermal power of the SF $\dot{Q}_{SF}$ is calculated by Eq. (22). The calculation of cosine losses $\cos(\theta_i)$, the incidence angle modifier $K(\theta_i)$ and the percentage of focused SF f_{foc} are discussed in detail by Hirsch et al. [14]. The nominal collector area A_{nom} and the direct normal irradiance G_{DNI} are varied during parametric study and the hour of the year.

$$\dot{Q}_{SF} = \eta_{SF} \cdot \cos(\theta_i) \cdot K(\theta_i) \cdot f_{foc} \cdot A_{nom} \cdot G_{DNI} \quad (22)$$

The efficiency of the SF η_{SF} is calculated by the efficiencies for optical losses η_{opt}, shading losses η_{shad}, mirror cleanness η_{clean}, wind losses η_{wind} and the field availability η_{avail}, as written in Eq. (23).

$$\eta_{SF} = \eta_{opt} \cdot \eta_{shad} \cdot \eta_{clean} \cdot \eta_{wind} \cdot \eta_{avail} \quad (23)$$

For the consideration of the SF heat loss $\dot{Q}_{SF,loss}$ during a yield calculation of a line focusing collector, Dudley et al. [15] proposed the following Eq. (24). The heat loss parameter $a_{HL} = 0.00047\ W\ m^{-2}K^{-2}$ for the used absorber is given by the work of Morin et al. [16]. The heat loss is calculated based on the quadratic temperature difference between the average absorber temperature T_{abs} and the temperature of the environment T_{env}.

$$\dot{Q}_{SF,loss} = a_{HL} \cdot (T_{abs} - T_{env})^2 \quad (24)$$

The technical design data of the solar thermal receiver, which provides saturated steam with a temperature of 143.6 °C and a pressure of 4 bar, is given by Table 1.

Table 1 – Technical design data for the solar thermal receiver.

Live steam pressure	4	bar
Live steam temperature	143.6	°C
Pressure drop receiver	1	bar
Loop length	600	m
Aperture width gross	5.76	m
Focal length	1.71	m
Optical efficiency	75	%

Please cite this article in press as: Seitz M, et al., Techno economic design of a solid oxide electrolysis system with solar thermal steam supply and thermal energy storage for the generation of renewable hydrogen, International Journal of Hydrogen Energy (2017), http://dx.doi.org/10.1016/j.ijhydene.2017.08.192

Latent heat thermal energy storage for the supply of saturated steam

For the extension of hydrogen production during the night time, a latent heat thermal energy storage (LHTES) is added with a thermal power of 2.3 MW (during charging and discharging) to the system (see Table 2). This TES is charged by saturated steam at 4 bar during the sunny hours of the day (day operational mode). During the night time, saturated steam at a pressure of 2.2 bar is forwarded to the SOEC (night operational mode). Due to the pressure range of the SOEC, an eutectic mixture of 67% by weight potassium nitrate (KNO_3) and 33% by weight lithium nitrate ($LiNO_3$), as discussed by Tamme et al. [17], was selected as the PCM.

The storage should provide a constant thermal power during charging and discharging. Such an active PCM system, called PCMflux, was introduced by the work of Pointner et al. [18]. The PCM is stored in separated aluminum containers. These containers are moved over a stationary aluminum fin. For a better heat transfer, an intermediate heat transfer fluid (HTF) is used. This HTF has a lower freezing point than the PCM. This TES system was demonstrated in lab scale by Pointner et al. [19] and is assumed for the storage calculation of the LHTES in this work.

Design of complete electrolysis system

For the calculation of the complete electrolysis system a simulation model (see Figs. 2 and 3) was created by the use of the software EBSILON®Professional. This system simulation model combines the sub-models of the SOEC, the SF, the TES and the compressor and drying stages. Several standard models for heat exchangers, pumps and compressors are used for modelling of the complete system behavior and the determination of the electrical own consumption. The design condition (day operational mode) of the electrolysis system is assumed for the production of hydrogen from saturated steam at 4 bar, which is directly produced by the SF. During low DNI periods, especially during the night, the parallel PCM-TES is discharged at a pressure of 2.2 bar (night operational mode). The four compressor and drying stages are designed for the discharge pressure of the TES at 2.2 bar. Therefore, both last stages are operated at part load at design conditions. It was assumed for all presented investigations that the electrical power of the SOEC is fixed at 10 MW at design conditions.

The assumed design parameters for the electrolysis system are provided in Table 3. The pressure loss of the SOEC is neglected due to the assumption that they have only small influence over the overall efficiency of the system. The terminal temperature difference (TTD) of the heat exchanger (HTX) is set to 10 K, which results in manageable areas for the heat exchange. The four compressor stages with intercoolers compress the hydrogen up to 30 bar.

By using the created system simulation model it is possible to calculate the pressure dependency of molar flow of produced hydrogen $\dot{n}_{H_2,prod}$ and the electrical power of the water electrolysis $P_{el,stack}$ (see Fig. 4, left). The molar flow of produced hydrogen, assuming a constant steam conversion rate, shows an increasing trend, if the operational pressure of the SOEC is decreased. Therefore, the electrical power of the SOEC stack also increases from 10 MW at a design pressure of 4 bar to 12 MW at an operational pressure of 1 bar.

It can be seen in Fig. 4 (right) that the enthalpy change $\Delta_r H_T$ is almost independent from the operating pressure of the SOEC. In fact, there is a shift from the product of temperature T and the entropy change of reaction $\Delta_r S_T$ to the Gibbs free energy change of reaction $\Delta_r G_T^0$. Due to the small energy changes, it can be concluded that the pressure influence on the water electrolysis reaction in the SOEC is small.

The efficiency of the electrolysis system η_{system} is calculated by Eq. (25) by the power flow of hydrogen, determined by the molar flow $\dot{n}_{H_2}$ and the higher heating (HHV) value of hydrogen $h_{HHV} = 285.84\ kJ\ mol^{-1}$ [20] divided by the thermal power of the receiver $\dot{Q}_{th,solar}$ and electrical power of the SOEC stack $P_{el,stack}$, of the feed stream heaters $P_{el,heater}$, of the pumps $P_{el,\ pump}$ and compressors $P_{el,comp}$. The power of the recuperation turbine $P_{el,recu}$ is considered to be negative, lowering the total energy demand of the electrolysis system.

$$\eta_{system} = \frac{\dot{n}_{H_2} \cdot h_{HHV}}{\dot{Q}_{th,solar} + P_{el,stack} + P_{el,heater} + P_{el,\ pump} + P_{el,comp} + P_{el,recu}} \tag{25}$$

In Table 4 the results from the system simulation model are shown for both day and night operational modes. The total energy demand for the night mode is higher than for the day mode. This is caused by the higher phase change enthalpy of water at 2.2 bar, the higher electrical consumption of the SOEC (depicted in Fig. 4, left) and the higher electrical consumption of the hydrogen compressors. The efficiencies for both day and night operational modes are 89.6% and 88.0%, respectively. It can be seen that the higher hydrogen molar flow which is produced during the night compensates the higher energy demand of the system almost completely, so that the difference in efficiency is only 1.6 %-pts.

The molar compositions (see Table 5) of the cathode inlet $\dot{n}_{cathode,in}$ and the anode inlet flow $\dot{n}_{anode,in}$ for both the day and the night operational mode. The molar composition of the outlet streams is due to the constant steam conversion rate of 75% constant for the day and the night operational mode.

Table 2 – Technical design data for the PCM storage [17].

Thermal power charging/discharging	2.3	MW
TTD for charging/discharging	10	K
Charging pressure	4	bar
Discharging pressure	2.2	bar
Melting temperature PCM	133	°C
Heat of fusion PCM	170	kJ/kg

Boundary conditions for hydrogen yield study

For the calculation of the hydrogen yield, several boundary conditions must be specified. Primarily, these are the direct normal irradiance (DNI) of the selected site and the electricity price for the electrolysis. In addition, the cost parameters for the estimation of the capital expenditures (CAPEX) and

Please cite this article in press as: Seitz M, et al., Techno economic design of a solid oxide electrolysis system with solar thermal steam supply and thermal energy storage for the generation of renewable hydrogen, International Journal of Hydrogen Energy (2017), http://dx.doi.org/10.1016/j.ijhydene.2017.08.192

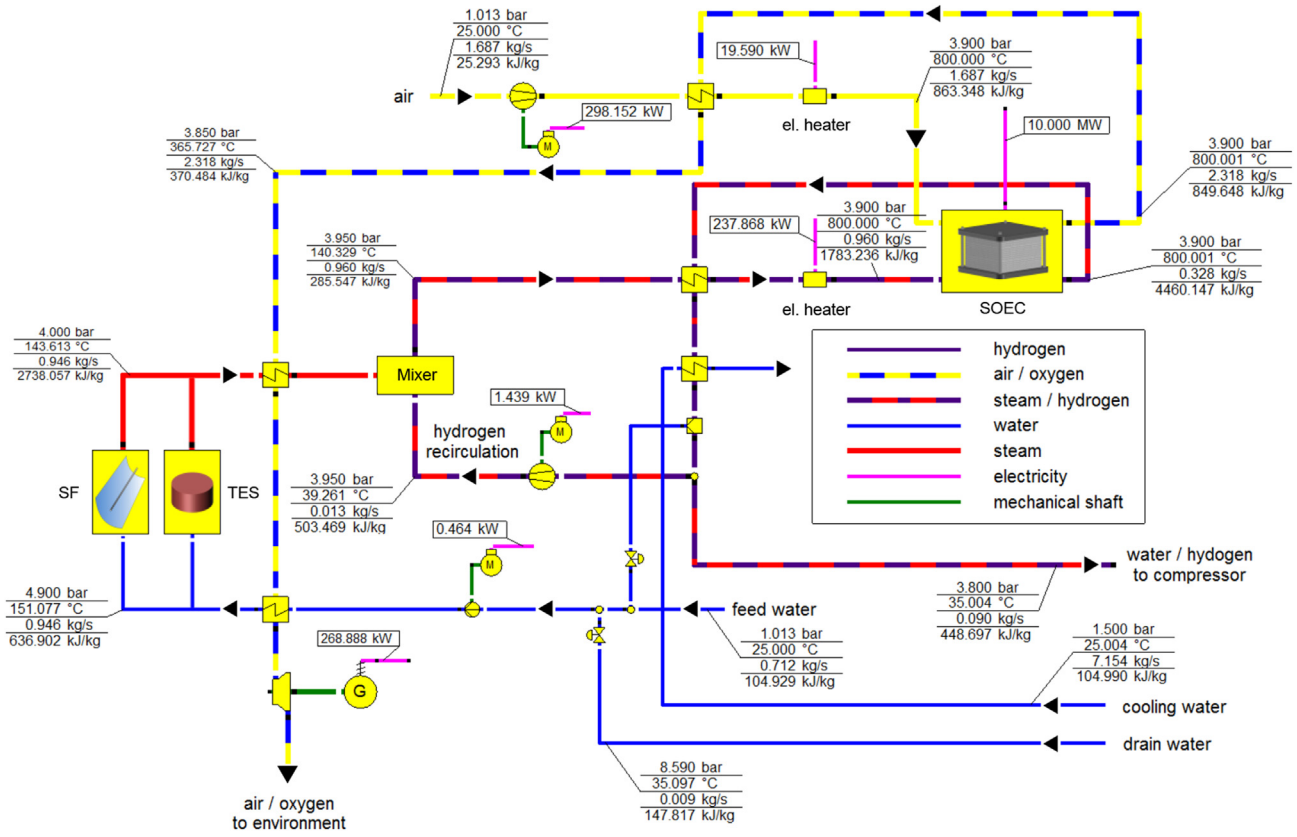

Fig. 2 – Simulation model of the electrolysis system with a 10 MW SOEC unit for the design point.

operational expenditures (OPEX) as well as the calculation of the annual hydrogen yield are determined.

Direct normal irradiance at plant site

For the calculation of the thermal power produced by the solar thermal receiver, a DNI for a typical metrological year (TMY) was used. The selected site is located near the city of Almería, Spain. This site was chosen because it provides sufficient solar resources in an area with sufficient infrastructure. Furthermore, abundant DNI data is available for this location. The measurements and techniques for the generation of the TMY dataset and the dataset itself are provided by Meyer and Schwandt [21]. The annual DNI sum of the dataset for the selected site, shown in Fig. 5, is about 2200 kWh/(m^2 a). This DNI is considered for each year of the annuity calculation of the SOEC plant.

It is assumed that the SOEC system is marketed at the Spanish day-ahead spot market. The merit order price curve for each hour of the next day in this market is generated by the operator of the Iberian electricity market (OMEL). The equilibrium price for each hour of the day is then published on the website of OMEL [22]. This price is generated by correlating electricity supply and demand of the electricity market.

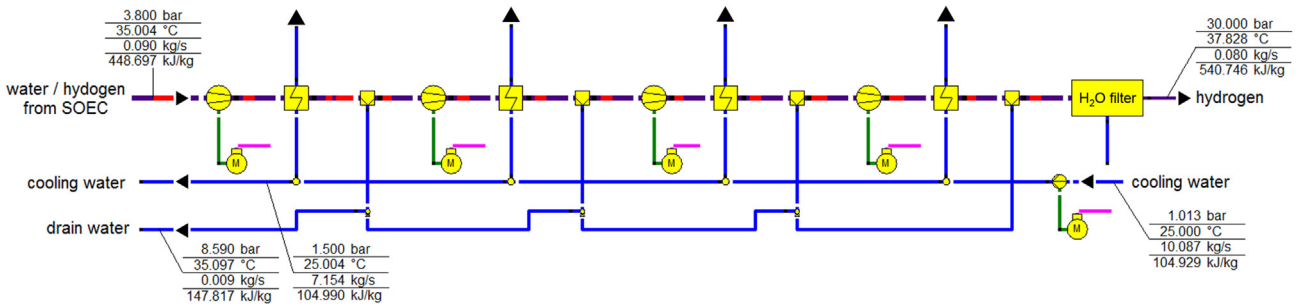

Fig. 3 – Simulation model of the four compressor and drying stages for the design point.

Please cite this article in press as: Seitz M, et al., Techno economic design of a solid oxide electrolysis system with solar thermal steam supply and thermal energy storage for the generation of renewable hydrogen, International Journal of Hydrogen Energy (2017), http://dx.doi.org/10.1016/j.ijhydene.2017.08.192

Table 3 – Technical design assumptions for the electrolyis system.

Electrical efficiency DC converter	98	%
Electrical efficiency motors	95	%
Mechanical efficiency motors	99	%
Electrical efficiency generator	99	%
Mechanical efficiency generator	99	%
Isentropic efficiency pumps	85	%
Isentropic efficiency fan	85	%
Isentropic efficiency turbine	90	%
TTD of recuperation HTX	10	K
TTD of inter-cooler HTX	10	K
Pressure drop HTX	50	mbar
Hydrogen storage pressure	30	bar

Table 4 – Results of the electrolyis system for the day and the night operational modes.

	Day	Night
Temperature SOEC (° C)	800	800
Operational pressure steam supply (*bar*)	4	2.2
Electrical power SOEC (MW)	10.0	11.1
Electrical own consumption (MW)	0.6	0.8
Thermal power electrolysis system (MW)	2.0	2.3
Total power input electrolysis system (MW)	12.6	14.2
Steam conversion rate (%)	75	75
Molar flow hydrogen ($kmol\ h^{-1}$)	142.1	157.0
Mass flow hydrogen ($kg\ h^{-1}$)	286.4	316.6
HHV output hydrogen (MW_{HHV})	11.3	12.5
Efficiency electrolysis system (%)	89.6	88.0

Table 5 – Molar compositions of the different streams at the cathode and the anode of the SOEC.

	Inlet	Outlet
Molar fraction hydrogen cathode	0.1	0.28
Molar fraction water/steam cathode	0.9	0.72
Molar fraction nitrogen anode	0.79	0.56
Molar fraction oxygen anode	0.21	0.44

For the study presented in this paper, the electricity prices of the last three years (see Fig. 6) were investigated. The electricity price is scattered between values close to 0 EUR/MWh and about 71 EUR/MWh, both in the year 2014. The year 2015 is characterized by high electricity prices between 16 EUR/MWh and 66 EUR/MWh. The dataset for the year 2016 includes the newest annual data for the investigated site at the time of the parametric study. The average daily electricity prices are between 5 EUR/MWh and 67 EUR/MWh. This results in an average electricity price of approximately 40 EUR/MWh. In the study, the year 2016 was selected for consideration, as it is assumed to represent the general trends in electricity prices well. There was no inflation or rise in electricity prices assumed for the presented study of the electrolysis system.

Operating modes of electrolysis system

The electrolysis system is operated in three different operating modes, shown in Table 6. The operational modes are determined by defined rules. If the DNI reaches a threshold of 300 KWh/m^2, the SF is in operation and the electrolysis system is operated in day mode (1). If there is a surplus of thermal energy, which is not consumed by the electrolysis system, the TES is charged up to its maximum thermal power (see Table 2) for the extension of hydrogen production during cloudy periods or night time (2). During the night operational mode of the electrolysis system, the TES is discharged at its design parameters (see Tables 2 and 4). During the rest of the annual hours, the system is operated at standby conditions (3).

Financial parameters for cost calculation

For the calculation of the hydrogen costs, the CAPEX and OPEX are estimated for each SF size and TES capacity of the investigated system. An adjustment of these cost parameters, in dependency of the size of the subcomponent, is not assumed. The specific parameters for the cost calculation are given in Tables 7 and 8. It should be noticed that the electrolyser price per kW_{el} mentioned in Table 7, which is of critical importance, is based on a cost study for manufacturing of SOFC power systems made by von Olshausen and Aldag [23] and Weimar et al. [24] and should be considered as a price forecast for the next 5–10 years.

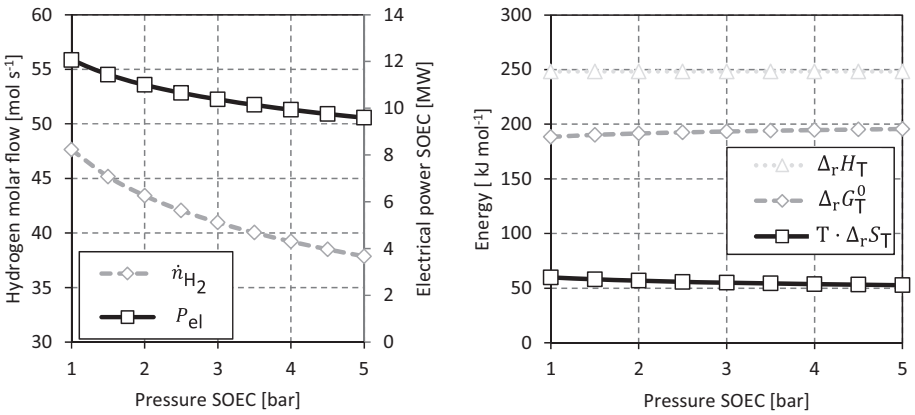

Fig. 4 – Pressure dependency (left) of the molar flow and the net electrical power of the SOEC system and (right) the enthalpy change, the Gibbs free energy change of reaction and the entropy change of the water electrolysis reaction.

Please cite this article in press as: Seitz M, et al., Techno economic design of a solid oxide electrolysis system with solar thermal steam supply and thermal energy storage for the generation of renewable hydrogen, International Journal of Hydrogen Energy (2017), http://dx.doi.org/10.1016/j.ijhydene.2017.08.192

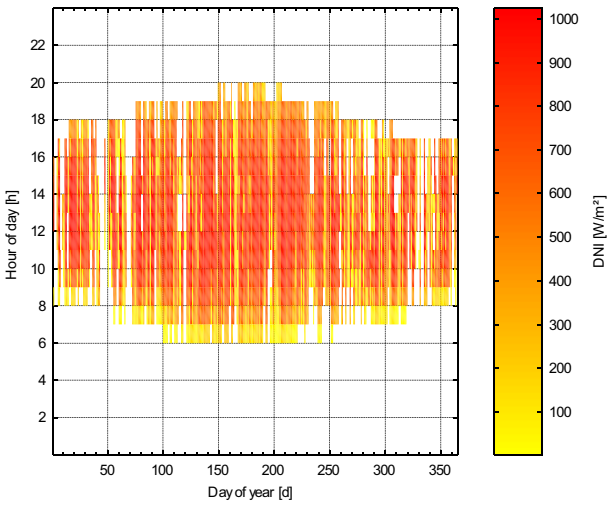

Fig. 5 – Hourly DNI dataset for the selected site near Almería, Spain.

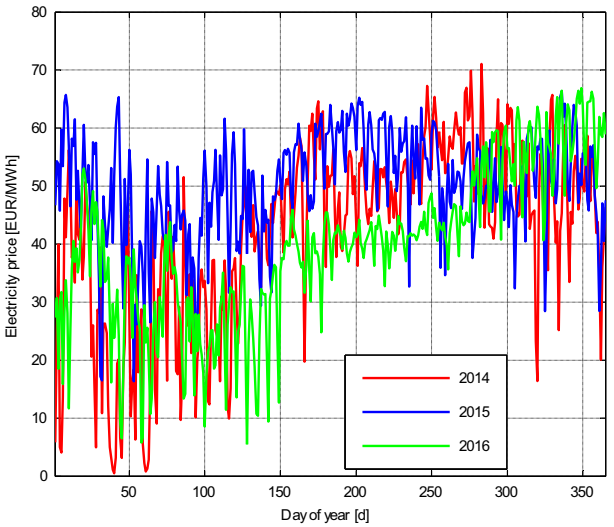

Fig. 6 – Medium daily electricity price of the day-ahead spot marked for the Spanish site [22].

Calculation of hydrogen costs

For the calculation of the LCOH, the annual amount of the CAPEX is calculated by the annuity factor f_{AN}. This factor is calculated in Eq. (26) by the payout time $n = 25$ years and the interest rate $i = 8$ % of the project.

$$f_{AN} = \frac{i^*(1+i)^n}{(1+i)^n - 1} \tag{26}$$

The LCOH are calculated by the annual costs C_{CAPEX}, C_{OPEX} and the electricity costs $C_{Electricity}$ during operational hours of the investigated year. These costs are divided through the molar mass flow of produced hydrogen $\dot{n}_{H_2,prod}$ and the higher heating value of hydrogen h_{HHV}. These energy specific costs are a good indicator for the comparison of different electrolysis layouts. The goal for an optimization of the system layout is to minimize the LCOH by finding the best configuration SF size and TES capacity.

$$C_{LCOH} = \frac{f_{AN} \cdot C_{CAPEX} + C_{OPEX} + C_{Electricity}}{\dot{n}_{H_2,prod} \cdot h_{HHV}} \tag{27}$$

Table 6 – Operational modes of the SOEC system used for the annual yield analysis.

Mode	Name	Solar field	Energy storage	Electrolyser
1	Day	on	charging	on
2	Night	off	discharging	on
3	Standby	off	off	off

Table 7 – Overview of specific cost parameters for the calculation of the CAPEX.

		Costs	Reference
Solar field	EUR/(m^2 aperture area)	240	[25]
Site preparation	EUR/(m^2 total area)	5	[26]
Factor A_{total}/A_{net}	–	4	[26]
Storage	EUR/KWh	80	[27]
Electrolyser	EUR/kW$_{el}$	1500	[23,24]
Project management	% der direct EPC costs	5	[26]
Profit	% of direct EPC costs	12	[26]
Project management owner	% of total EPC costs	3	[26]
Other costs owner	% of total EPC costs	3	[26]
Grid connection	10^6 EUR	5	[26]

Results and discussion

In a first step, an optimization of the baseline scenario with a TES is presented. In comparison with these first LCOH results, a system layout without TES is introduced for the discussion of the TES impact to the LCOH. Finally, a sensitivity study is shown for the determination of the four most relevant cost components of the cost structure of the electrolysis system.

Table 8 – Overview of the specific cost parameters for the calculation of the OPEX.

		Costs	Reference
Maintenance solar field	(% of SF-CAPEX)/a	0.5	[26]
Maintenance storage	(% of TES-CAPEX)/a	0.3	[26]
Maintenance electrolyser	(% of EL-CAPEX)/a	1	[26]
Management maintenance	(% of direct EPC costs)/a	0.15	[26]
Insurance	(% of direct EPC costs)/a	12	[26]
Water costs	EUR/m^3	0.5	[26]
Labor costs (average)	EUR/a	48,000	[28]
Staff (fix)	–	10	[28]
Staff (variable)	1/(1000 m^2 aperture area)	0.03	[28]
Ground lease	EUR/(m^2 total area a)	0.2	[26]

Please cite this article in press as: Seitz M, et al., Techno economic design of a solid oxide electrolysis system with solar thermal steam supply and thermal energy storage for the generation of renewable hydrogen, International Journal of Hydrogen Energy (2017), http://dx.doi.org/10.1016/j.ijhydene.2017.08.192

Optimization of the baseline scenario with storage

The LCOH of the electrolysis system are calculated for 961 different configurations in dependency of the two main design parameters of the discussed system. These parameters are the TES discharge hours and the number of collector loops of the SF with the following parameter ranges:

- TES discharge hours: 0–30 h in 1 h steps
- Number of collector loops: 1.5–9 in 0.25 steps.

The LCOH shape a surface with a global minimum in-between the selected parameters range of the parametric study. For the selected Spanish site near Almería and the electricity price of 2016, the result of the parametric study is depicted in Fig. 7. The lowest LCOH of 0.11 EUR/kWh$_{HHV}$ or 4.30 EUR/kg are calculated for an electrolysis system with a discharge time of 11 h and 4.25 collector loops. This requires a thermal storage capacity of 25.6 MWh and a total gross aperture of 14,688 m^2.

Inappropriate system configurations, e.g. with long TES discharge hours and few collector loops, are characterized by high LCOH. These configurations are not suitable for an economical design of the electrolysis system. The proposed cost structure leads to a relatively large local minimum and enables several configurations with almost identical LCOH. For the further investigations in this paper, the system with the lowest LCOH was selected.

Comparison of the baseline scenario with and without storage

A direct comparison of an electrolysis system with and without a TES shows the impact of the TES to the LCOH. In Fig. 8, the operational hours for both discussed systems are depicted. Without a TES, the system is operated for about 2440 h in the SF operational mode. The rest of the year, mainly the night and the cloudy hours of the year, the system is in standby operational mode. The TES of the baseline scenario, discussed above, rises the operational hours in SF and TES mode to 4910 h. The number of hours in the standby operational mode is decreased by about 39% from 6320 h to 3850 h.

Due to the integration of the TES with a thermal capacity of 25.6 MWh, the production hours are extended by about 50% (see Table 9). This results in a reduction of the system LCOH by about 34% from 0.16 EUR/kWh to 0.11 EUR/kWh, based on the HHV of hydrogen.

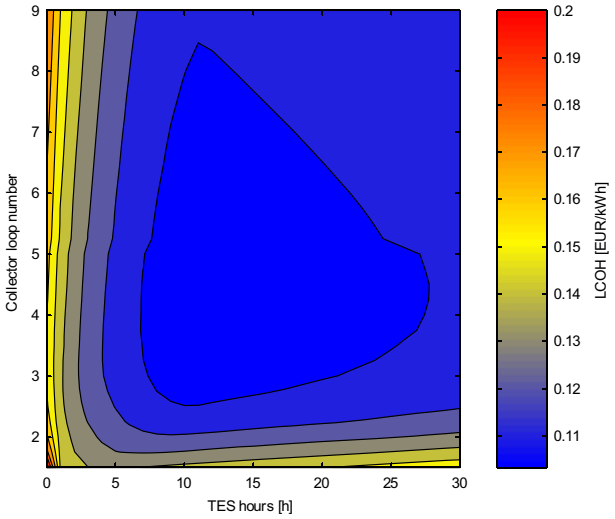

Fig. 7 – Calculation of LCOH in dependency of the number of collector loops and the TES discharge hours of the baseline scenario.

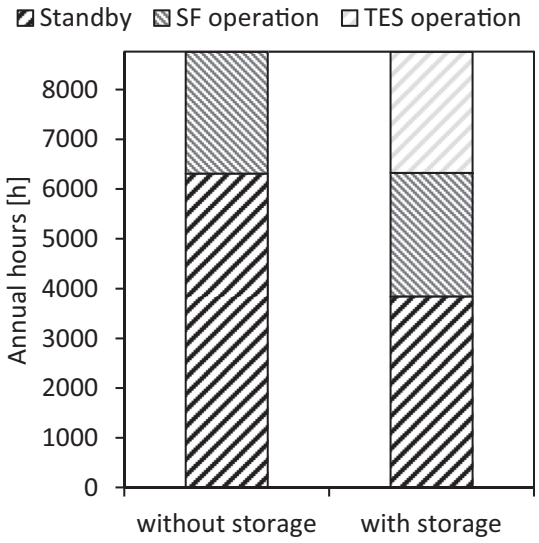

Fig. 8 – Distribution of the operational hours for an optimized electrolysis system with and without a TES.

Sensitivity study of CAPEX cost structure

In a last step of the presented study, the sensitivity of the discussed electrolysis system with TES is calculated. For this, the four main components of the systems cost structure are selected. The CAPEX costs assumptions for the TES, the SF, the electrolyser and the electricity costs are varied from −20% to +20%. For the determination of the sensitivity, the percentage change of the LCOH, caused by the respective component of the cost structure, is evaluated.

The results of the sensitivity study are depicted in Fig. 9. The calculated specific costs for the 100% case are given in Table 7 and Fig. 6. In case of the electricity price, each hour value of the year is scaled for the sensitivity study. If the CAPEX of the TES and the SF are changed by ± 20%, the LCOH is only modified by about ± 0.9% and ± 1.5%, respectively. The

Table 9 – Results of the comparsion of the baseline scenario with and without a TES.

		Without storage	With storage
TES capacity	[MWh]	–	25.6
Production hours	[h]	2440	4910
LCOH	[EUR/kWh]	0.16	0.11

Please cite this article in press as: Seitz M, et al., Techno economic design of a solid oxide electrolysis system with solar thermal steam supply and thermal energy storage for the generation of renewable hydrogen, International Journal of Hydrogen Energy (2017), http://dx.doi.org/10.1016/j.ijhydene.2017.08.192

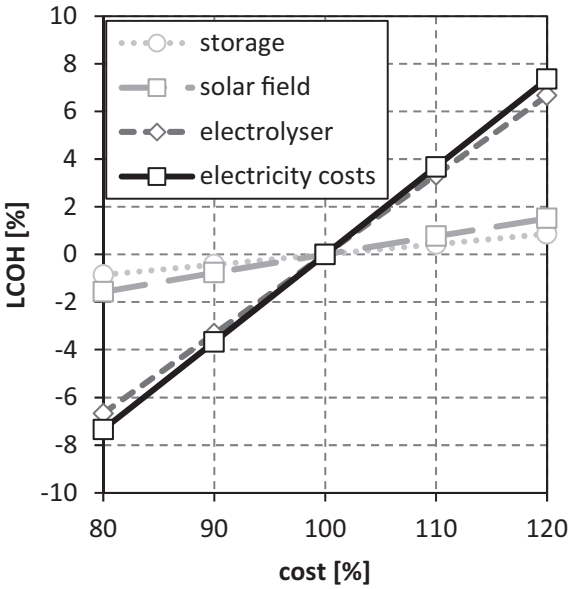

Fig. 9 – Cost sensitivity of the LCOH for the CAPEX of the subsystems storage, solar field, electrolyser and the electricity costs.

main influences on the LCOH are the CAPEX for the electrolyser and the electricity costs with ± 6.7% and ± 7.3%, respectively.

Conclusions

This paper presents a techno economic investigation of a solar thermal powered electrolysis system with an integrated TES for medium- and long-term storage of renewable energy. The conducted calculation of the LCOH shows a minimum at about 0.11 EUR/KWh, with a TES discharge time of 11 h and a total SF gross aperture of 14,688 m^2. The results of the study also show that the TES reduces the LCOH by about 34% and extends the annual hydrogen production time by about 50%.

It can be shown with the sensitivity results that the main cost reduction potential of the system is hidden in the CAPEX costs of the electrolyser, which is by far the most expensive component of the system. For that reason, the research on SOEC has to be continued. The second cost reduction potential is the electricity cost, for the operation of the water electrolysis and the own consumption for pumps and compressors. If the price of renewable electricity decreased in the medium term, the LCOH of renewable hydrogen would also decline.

Finally, the results show a positive impact of the integration of a TES with a PCM material, which causes a lower water pressure during the discharge process of the TES. The pressure difference leads to a very small decrease of the conversion efficiency of the renewable electricity to hydrogen, which is partially compensated by the higher hydrogen production of the SOEC during the TES discharge mode. This is caused by the small influence of the steam pressure on the water electrolysis. It can be shown that the presented PCM-TES concept is a promising solution for the extension of hydrogen production with solar powered SOEC systems, which should be thoroughly investigated in further research projects.

Acknowledgements

The presented work was partly funded by the German Federal Ministry for Economic Affairs and Energy. The authors are responsible for the content of this publication.

REFERENCES

[1] Gahleitner G. Hydrogen from renewable electricity: an international review of power-to-gas pilot plants for stationary applications. Int J Hydrogen Energy 2013;38:2039–61. http://dx.doi.org/10.1016/j.ijhydene.2012.12.010.

[2] Nechache A, Cassir M, Ringuedé A. Solid oxide electrolysis cell analysis by means of electrochemical impedance spectroscopy: a review. J Power Sources 2014;258:164–81. http://dx.doi.org/10.1016/j.jpowsour.2014.01.110.

[3] Henke M, Willich C, Kallo J, Friedrich KA. Theoretical study on pressurized operation of solid oxide electrolysis cells. Int J Hydrogen Energy 2014;39:12434–9. http://dx.doi.org/10.1016/j.ijhydene.2014.05.185.

[4] Sanz-Bermejo J, Muñoz-Antón J, Gonzalez-Aguilar J, Romero M. Part load operation of a solid oxide electrolysis system for integration with renewable energy sources. Int J Hydrogen Energy 2015;40:8291–303. http://dx.doi.org/10.1016/j.ijhydene.2015.04.059.

[5] Monnerie N, von Storch H, Houaijia A, Roeb M, Sattler C. Hydrogen production by coupling pressurized high temperature electrolyser with solar tower technology. Int J Hydrogen Energy 2016;42:13498–509. http://dx.doi.org/10.1016/j.ijhydene.2016.11.034.

[6] Joshi AS, Dincer I, Reddy BV. Solar hydrogen production: a comparative performance assessment. Int J Hydrogen Energy 2011;36:11246–57. http://dx.doi.org/10.1016/j.ijhydene.2010.11.122.

[7] Alzahrani AA, Dincer I. ScienceDirect Thermodynamic and electrochemical analyses of a solid oxide electrolyzer for hydrogen production. Int J Hydrogen Energy 2017;42:21404–13. http://dx.doi.org/10.1016/j.ijhydene.2017.03.186.

[8] Petipas F, Brisse A, Bouallou C. Model-based behaviour of a high temperature electrolyser system operated at various loads. J Power Sources 2013;239:584–95. http://dx.doi.org/10.1016/j.jpowsour.2013.03.027.

[9] Fu Q, Mabilat C, Zahid M, Brisse A, Gautier L. Syngas production via high-temperature steam/CO_2 co-electrolysis: an economic assessment. Energy Environ Sci 2010;3:1382. http://dx.doi.org/10.1039/c0ee00092b.

[10] Rivera-Tinoco R, Mansilla C, Bouallou C. Competitiveness of hydrogen production by High Temperature Electrolysis: impact of the heat source and identification of key parameters to achieve low production costs. Energy Convers Manag 2010;51:2623–34. http://dx.doi.org/10.1016/j.enconman.2010.05.028.

[11] Udagawa J, Aguiar P, Brandon NP. Hydrogen production through steam electrolysis: model-based steady state performance of a cathode-supported intermediate temperature solid oxide electrolysis cell. J Power Sources 2007;166:127–36. http://dx.doi.org/10.1016/j.jpowsour.2006.12.081.

Please cite this article in press as: Seitz M, et al., Techno economic design of a solid oxide electrolysis system with solar thermal steam supply and thermal energy storage for the generation of renewable hydrogen, International Journal of Hydrogen Energy (2017), http://dx.doi.org/10.1016/j.ijhydene.2017.08.192

[12] SCHOTT Solar CSP GmbH. SCHOTT PTR®70 receivers, Dataheet. 2013.
[13] Feldhoff JF, Hirsch T, Pitz-Paal R, Valenzuela L. Analysis and potential of once-through steam generators in line focus systems – final results of the DUKE project. AIP Conf Proc 2016:1734. http://dx.doi.org/10.1063/1.4949194.
[14] Hirsch T, Dersch J, Fluri T, García-Barberena J, Giuliano S, Hustig-Diethelm F, et al. SolarPACES guideline for bankable STE yield assessment. 2017.
[15] Dudley VE, Kolb GJ, Mahoney AR, Mancini TR, Matthews CW, Sloan M, et al. Test results: SEGS LS-2 solar collector. Technical Report SAND94-1884. Sandia Natl Lab; 1994.
[16] Morin G, Dersch J, Platzer W, Eck M, Häberle A. Comparison of linear fresnel and parabolic trough collector power plants. Sol Energy 2012;86:1–12. http://dx.doi.org/10.1016/j.solener.2011.06.020.
[17] Tamme R, Bauer T, Buschle J, Laing D, Müller-Steinhagen H, Steinmann W-D. Latent heat storage above 120°C for applications in the industrial process heat sector and solar power generation. Int J Energy Res 2008;32. http://dx.doi.org/10.1002/er.1346.
[18] Pointner H, Steinmann WD, Eck M. Introduction of the PCM flux concept for latent heat storage. Energy Procedia 2014;57:643–52. http://dx.doi.org/10.1016/j.egypro.2014.10.219.
[19] Pointner H, Steinmann WD. Experimental demonstration of an active latent heat storage concept. Appl Energy 2016;168:661–71. http://dx.doi.org/10.1016/j.apenergy.2016.01.113.
[20] Grote K-H, Feldhusen J, editors. Dubbel – Taschenbuch für den Maschinenbau (in German). 23rd ed. Berlin Heidelberg: Springer-Verlag; 2011.
[21] Meyer R, Schwandt M. Documentation of meteorological data sets delivered together with the SolarPACES guideline for bankable STE yield assessment. 2017.
[22] OMI-Polo Español S.A. Daily market hourly price n.d. http://www.omel.es/files/flash/ResultadosMercado.swf [Accessed January 16 2017].
[23] von Olshausen C, Aldag N. Power-to-X mit reversibler SOC-Dampfelektrolyse. 7. Dtsch. Wasserst. Congr. 2016, Berlin. 2016.
[24] Weimar M, Chick L, Gotthold D, Whyatt G. Cost study for manufacturing of solid oxide fuel cell power systems. 2013.
[25] Dieckmann S, Dersch J, Giuliano S, Puppe M, Lüpfert E, Hennecke K, et al. LCOE reduction potential of parabolic trough and solar tower technology until 2025. 2016. p. 3–10.
[26] Hirsch T, Yildiz E. CSPBankability project report: draft for an appendix O – cost structures to the SolarPACES guideline for bankable STE yield assessment. 2017.
[27] Seitz M, Johnson M, Hübner S. Economic impact of latent heat thermal energy storage systems within direct steam generating solar thermal power plants with parabolic troughs. Energy Convers Manag 2017;143:286–94. http://dx.doi.org/10.1016/j.enconman.2017.03.084.
[28] Richter C. Abschlussbericht EFCOOL-Wassereffiziente Kühlung solarthermischer Kraftwerke (in German). 2007.

Please cite this article in press as: Seitz M, et al., Techno economic design of a solid oxide electrolysis system with solar thermal steam supply and thermal energy storage for the generation of renewable hydrogen, International Journal of Hydrogen Energy (2017), http://dx.doi.org/10.1016/j.ijhydene.2017.08.192